Instantaneous flow rate measurements for strong pulsated flows. Application to GDI swirl injectors.

G. DELAY[1], R. BAZILE[1], L. BEN[1], E.CID[1], G. CHARNAY[1], J. BOREE[2] & H.J. NUGLISCH[3].

1. Institut de Mécanique des Fluides de Toulouse, France
2. Laboratoire d'Etudes Aérodynamiques, Poitiers, France
3. SIEMENS Automotive-VDO Toulouse, France

1. Abstract

We are presenting here an instantaneous flow rate measurement method [1, 2, 4, 5 & 6] particularly well suited to the study of pulsated flows taking place in feeding systems of car injectors. It is based upon non-intrusive Laser Doppler Anemometry (LDA) velocity measurements at the centerline of a Pyrex pipe feeding the injector. The laminarity and the parralelism flow criterion can be easily fullfilled in the context of GDI (hollow cone spray). The issue, besides the development of such a technique, is to help for injectors' sprays transient analysis (penetration length, angle, atomisation) and loop pressure regulation. This will be done by coupling in real-time flow rate determination before the injector (Laser Doppler Anemometry and flow rate rebuilding method) and spray development analysis after the injector (Particle Image Velocimetry). The injection frequencies have been set from 1 to 60 Hz, pulse width varying from 1 to 50 % of the period, then including the functioning range of a real injector (10-60 Hz, 1-5 ms). The measured flow rates are always inferior to 1 g/s (1.3 ml/s).

Symbols :

U : velocity ;
r : radial coordinate ;
R : inner radius of the Pyrex tube ;
ϕ_{int}, ϕ_{ext} : inner and outer pipe diameter ;
ω : angular velocity ;
ρ : fluid density ;
ν : kinematic viscosity ;
$\delta = \sqrt{\frac{2\upsilon}{\omega}}$: Stokes' length ;
c : Fourier coefficients ;
p' : Lambossy pressure gradients ;
J : Bessel function ;
$Ta = R\sqrt{\frac{\omega}{\upsilon}}$: Taylor number.

2. Introduction

Measuring instantaneous flow rate and pressure gradients is critical for the design of injection system. Indeed, injection frequencies (from 10 to 60 Hz for an injector) and short injection durations (inferior to 5 ms) generate periodical transient flows with great oscillation magnitude. As a result, the determination of such flows can be of a great help in the design of the injection loop (pipes lengths and diameters, rail volume, materials and pressure regulation). Moreover, knowing instantaneous flow rates allows to transpose analysis of steady liquid spray development to transient ones. Indeed, many air entrainment studies use the mean flow rate as a key, but of course, time-constant parameter. This paper deals with the validation of a rebuilding method [1, 2, 4, 5 & 6] applied to low and medium pressure injector (3.5 and 80 bar), finishing with some considerations about coupling those results with air entrainment.

3. Measurement method

It has been introduced in 1952 by Paul Lambossy [3], a physiologist, with a view to measuring arterial pressure with mercury manometers and then by Durst & Ismailov [1, 2, 4, 5, 6] to study instantaneous flow rates through injectors.

The velocity distribution of a pulsed flow is indeed corresponding to a pressure gradient defined by $\frac{\partial P}{\partial z} = -\rho\left[p'_0 + (p'_1 e^{i\omega t} + C.C.)\right]$ (p' pressure gradient, CC complex conjugate) and can be expressed by a stationary part on which is added an oscillating part, depending on the pulsation of the pressure gradient :

$$U(r,t) = \frac{R^2 p'_0}{4\upsilon}\left[1 - \left(\frac{r}{R}\right)^2\right] + \frac{p'_1}{\omega} i e^{i\omega t}\left[\frac{J_0\left(i^{3/2} r\sqrt{\frac{\omega}{\upsilon}}\right)}{J_0\left(i^{3/2} R\sqrt{\frac{\omega}{\upsilon}}\right)}\right] + C.C. \qquad (1)$$

We can then introduce the Taylor number, $Ta = R\sqrt{\frac{\omega}{\upsilon}}$, that characterises the competition between viscous and transient effects, giving information on the shape of the velocity distribution. Hence, for Ta>>1, ie. when transient effects are far more important than viscous ones, we can assume that the flow is a solid-like one whereas a Ta<<1 flow would be closer to a parabola (Poiseuille flow). This is illustrated on figure 1 with four velocity distributions computed with different injection frequencies, putting on light the frequency-dependant velocity distribution.

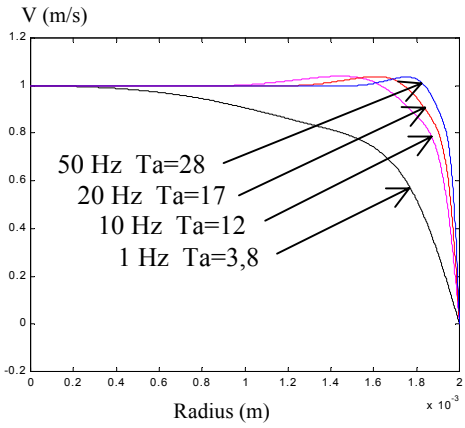

Fig. 1 : Velocity distribution as a function of frequency

(1) can then be written as follows :

$$U(r,t) = \frac{R^2 p'_0}{4\upsilon}\left[1 - \left(\frac{r}{R}\right)^2\right] + \frac{p'_1}{\omega} i e^{i\omega t}\left[\frac{J_0\left(i^{3/2} Ta\,\frac{r}{R}\right)}{J_0\left(i^{3/2} Ta\right)}\right] + C.C. \qquad (2)$$

This method can be applied to flows generated by a superposition of periodical pressure gradients that can be written according to the Fourier formalism :

$$\frac{\partial P}{\partial z} = -\rho\left[p'_0 + \sum_{n=1}^{\infty}\left(p'_n e^{in\omega t} + C.C.\right)\right] \qquad (3)$$

With the following reduced Navier-Stockes equation for an axisymetric, laminar (see at the end of this paragraph) and parallel flow :

$$\rho\frac{\partial U}{\partial t} = -\frac{\partial P}{\partial z} + \mu\left(\frac{1}{r}\frac{\partial}{\partial r}\left(r\frac{\partial U}{\partial r}\right)\right) \qquad (4)$$

Transient effects — Pressure gradient — Viscous effects

Here we see that this equation is a linear one and, following Lambossy's way, it is possible to evaluate the entire velocity distribution with ($Ta_n = R\sqrt{\frac{\omega n}{\upsilon}}$):

$$U(r,t) = \frac{R^2 p'_0}{4\upsilon}\left[1 - \left(\frac{r}{R}\right)^2\right] + \sum_{n=1}^{\infty}\left(\frac{p'_n}{n\omega} i e^{in\omega t}\left[\frac{J_0\left(i^{3/2} Ta_n\,\frac{r}{R}\right)}{J_0\left(i^{3/2} Ta_n\right)} - 1\right] + C.C.\right) \qquad (5)$$

The volumetric flow rate can be calculated by integration of U(r,t) given by (5). We can infer the following expression (6), p'_0 and p'_n unknown pressure gradients :

$$Q(t) = 2\pi\int_0^R U(r,t)rdr = \frac{\pi R^2}{2}\left(\frac{R^2 p'_0}{4\nu} + \sum_{n=1}^{\infty}\left(\frac{p'_n}{n\omega} ie^{in\omega t}\left[\frac{4i^{1/2}J_1\left(i^{3/2}Ta_n\right)}{Ta_n J_0\left(i^{3/2}Ta_n\right)} - 2\right] + C.C\right)\right) \quad (6)$$

The evaluation of the flow rate is yet impossible because the p'_n coefficients are still unknown. However, by considering the centreline velocity, (5) becomes with r=0:

$$U(r=0,t) = \frac{R^2 p'_0}{4\upsilon} + \sum_{n=1}^{\infty}\left(\frac{p'_n}{n\omega} ie^{in\omega t}\left[\frac{1}{J_0\left(i^{3/2}Ta_n\right)} - 1\right] + C.C.\right) \quad (7)$$

U(r=0,t) can be written following Fourier formalism : $U(r=0,t) = \frac{c_0}{2} + \sum_{n=1}^{N\,exp}\left(c_n e^{in\omega t} + C.C.\right)$ (8)

Finally, by matching velocities expressions (7) and (8), we get the p'_0 and p'_n values :

$$\frac{c_0}{2} = \frac{R^2 p'_0}{4\upsilon} \quad et \quad c_n = i\frac{p'_n}{n\omega}\left[\frac{1}{J_0\left(i^{3/2}Ta_n\right)} - 1\right] \quad (9)$$

This analytical resolution can only be applied in the case of laminar and parallel flows. Flows have to verify, not the classical Reynolds criterion based on the pipe diameter for steady flows, but a Stokes' length based one : $Re_\delta = \frac{U\delta}{\nu} = \frac{U\sqrt{\frac{2\upsilon}{\omega}}}{\nu} \leq 550$ [1, 7, 8 , 9, 10, 11]

It is yet possible to determine instantaneous volumetric flow rate only using centreline velocity measurements. Data processing, here thanks to a Matlab program, will perform the required Fast Fourier Transform (FFT) operation of the velocity signal measured during N_{exp} cycles. Matching of Fourier and Lambossy coefficients will lead first to the determination of the whole velocity distribution, and then of the instantaneous flow rate.

4. Experimental setup

To measure velocities (Laser Doppler Anemometry, figure 2), we have inserted before the injector a Pyrex tube (figures 3a & 3b, ϕ_{ext}=12mm, ϕ_{int}=4mm, L=100 and then 500mm) mounted on a 3D positionning device (precision of 10 µm). The laser used is a Spectra Physics one (Argon 2020, 4W) delivering a 514.5 nm wavelength laser beam, split, shifted in frequency and focused in the measurement volume. The car calculator drives the injector (injection frequency and duration) and evaluates the camshaft angle corresponding to the measurement arrival time, leading to a cyclic phenomena approach. The "shot to shot" variations are not taken into account, the rms of the phase averaged signal being however inferior to 5%.

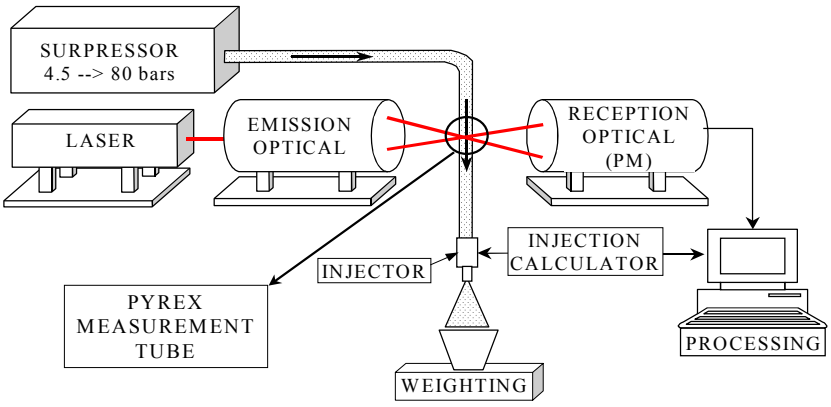

Fig. 2 : Experimental setup

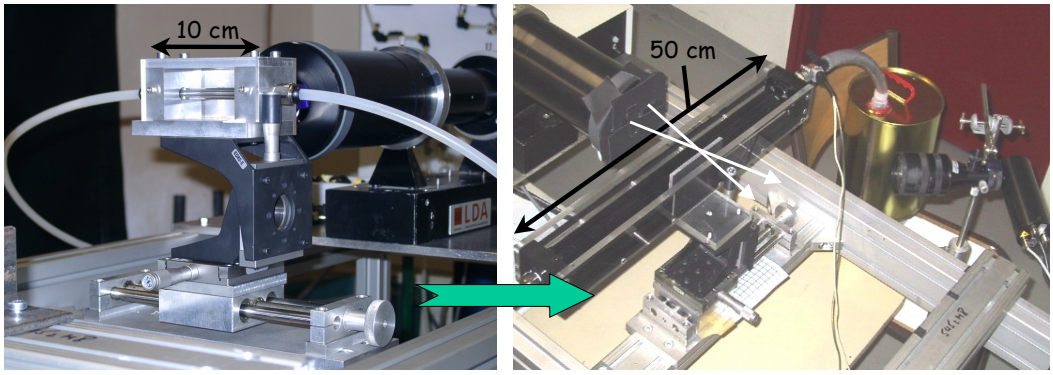

Fig. 3a & b : Evolutions of the Pyrex tube in its Plexiglas protecting box, mounted on a 3D motion module (length from 100 to 500 mm and wall anodisation)

To ensure a sufficient data rate, polymer particles have been used as seeding of the flow (ρ_{fluid}=763 kg/m^3, ν_{fluid}=1.67e^{-6} m^2/s). Their diameter (inferior to 5µm with appropriate filtration) and density (1200 kg/m^3) are well fitted with the flows we want to study here, their response time being far smaller than the characteristic time of studied flows :

$$\tau_{particle} = \left(\frac{\rho_{particle}}{\rho_{fluid}} + \frac{1}{2} \right) * \frac{D^2}{18 \upsilon_{fluid}} = 1.67e^{-6} \text{ s.}$$

The velocity measurements are then computed thanks to phase averaging and velocity distribution rebuilding, giving finally access to the instantaneous flow rate. The validation is yet realised thanks to weightings and comparisons between rebuilt and LDA-measured velocity distributions (see later on).

5. Experimental results

First of all, here are some results proving that the coupling between LDA velocity measurements and the rebuilding theory is a good way to determine instantaneous flow rate in the pipe feeding the injector.

Before going further on, let us have a look at the shape of a typical rebuilt instantaneous flow rate, injection frequency being of 50 Hz and injection duration of 2 ms (figure 4). The square line stands for the control signal driving the injector and we can here see the great magnitude of flow rate oscillations compared to injector static flow rate. We can then define four phases, whatever the injector, the frequency, the duration or the injection pressure is.

First, the opening phase (A), corresponding to the needle lift time of the injector, is sharper as the injector opens faster, it is quite a constant characteristic time of the injector. It is followed by the injection (B), whose duration is determined by the user. Its shape is far from a simple square signal because of the water hammer effect that induces oscillations which frequencies and magnitudes are function of the loop geometry and fluid properties. Then, symetrically to the opening, the closing phase (C), also characteristic of the injector, is followed by a damping of the oscillations (D).

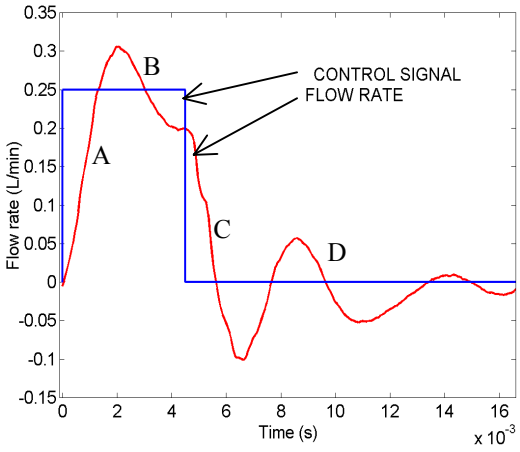

Fig. 4 : Injection signal and associated flow rate (low pressure).

By superposing various injection duration signals, we verify that opening and closing are characteristic of the injector thanks to their perfect similarity (figure 5). Moreover, each signal is affected by the same pressure wave 7.6 ms after the beginning of injection because of the water hammer effect created at the opening.

By synchronising closings instead of openings, the same pressure wave, with an opposite magnitude, appears again 7.6 ms after the sudden change of boundary conditions (ie. the closing). The length of the loop being 4.2 m, we can infer that the pressure wave celerity is close to 1100 m/s. The pressure wave presence can also be found 16 ms after opening (or closing) during its second passage.

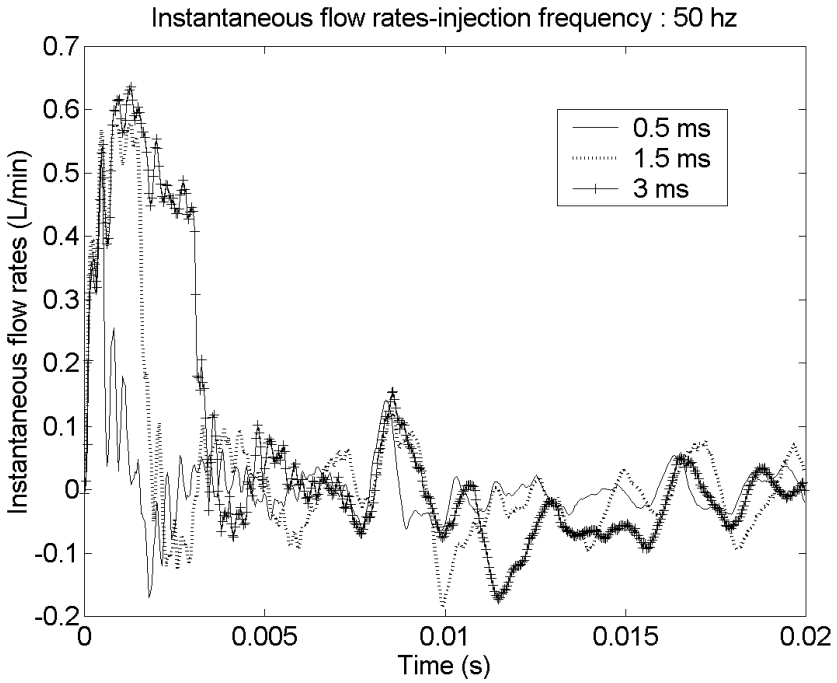

Fig 5 : Instantaneous flow rate at 50 Hz for various injection durations Synchronisation at the opening.

One can notice that injection oscillations can reach more than 20% of the mean value, that is to say a potential variation of 45% of the kinematic energy given, first to the liquid phase of the spray, and then to the ambient air. The spray geometry (angle and penetration length) could also be modified by this unsteady flow rate.

To evaluate the accuracy of LDA measurements, here is a cumulated repartition of centerline velocity measurements achieved during an injection phase (figure 6).

One can see that measurements are not very dispersed (RMS inferior to 4 %) and that no preferential velocity acquisition bias is detected.

Indeed, the linear evolution of the cumulated repartition slope in the vincinity of the mean value traduces the equiprobabilty of measuring velocities with various magnitudes.

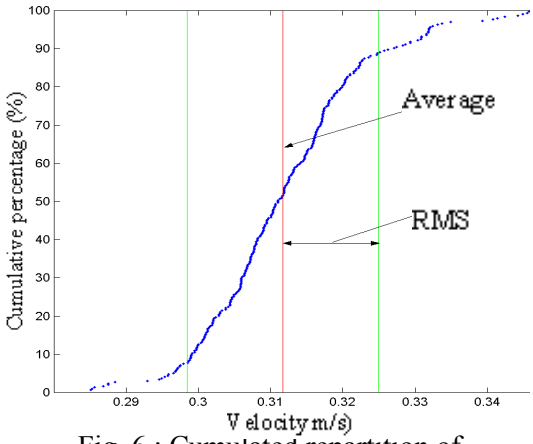

Fig. 6 : Cumulated repartition of measurements done during injection

Unstationnary flows are well spatially and temporally determined (figure 7). There is a good match between rebuilt and laser-based velocity distributions on a more than 90% of the radius, whatever the injection phase.

The gaps close to the wall are due to superposition of the laser-induced measurement volume with the Pyrex tube wall.

It is also interesting to notice the occurrence of full reversed flows during closing phases, and even partially reversed ones during calming down phases.

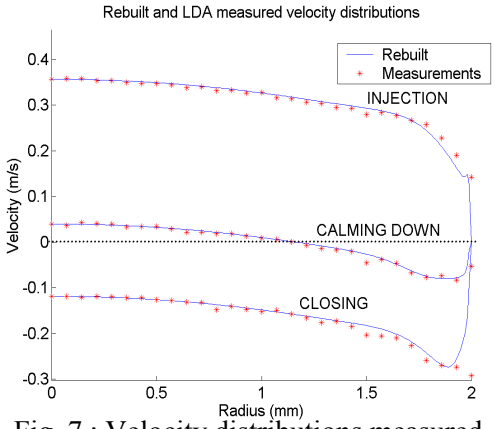

Fig. 7 : Velocity distributions measured by LDA (*) and rebuilding theory

To go further on with the water hammer effect, here is a proof of its symetrical behaviour and of its dependance on the geometrical and physical parameters of the injection loop (figure 8).

Indeed, one can see that by duplication, symetry and superposition of the opening signal at the closing, this new signal matches very well with the closing one.

Moreover, various frequencies can be detected. The higher one, mostly present during the 2 ms following opening and closing, is generated by the Pyrex measurement tube.

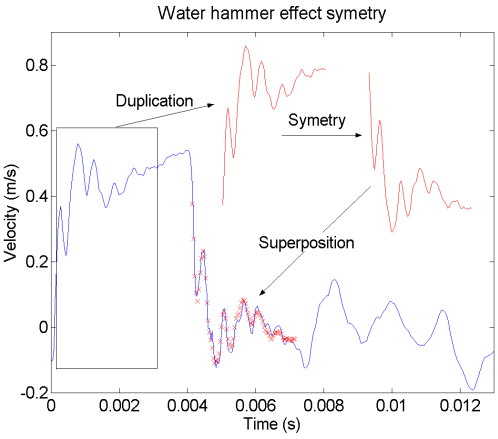

Fig. 8 : Water hammer effect symmetry

The lower one is due to the pipe located between the Pyrex tube and the surpressor. As it is less stiff than the Pyrex tube, the oscillation frequency is lower. Indeed, the celerity of a pressure wave in non-rigid pipe can be written as

$$a = \sqrt{\frac{1}{\rho\left(\frac{D}{eE} + \frac{1}{\chi}\right)}}$$

With :
- a : pressure wave celerity (m/s),
- ρ : density of the fluid (kg/m^3),
- D and e : diameter and thickness of the pipe (m),
- E : Young modulus of the pipe (Pa),
- χ : liquid compressibility (Pa)

A stiffer pipe (greater E) will then generate faster pressure wave, ie. higher oscillation frequencies. The accoustic coupling of two pipes of different diameters allows to found the main accoustic modes, different from the ones generated by the considered pipes alone [13].

Up to now, there is only one fast and simple way (excluding the too long LDA velocity distribution measurement) to check the validity of this theory : the mean flow rate passing through the injector.

Figure 9 shows the accuracy of the rebuilding method by comparing weighted and rebuilt flow rates. The error is always inferior to 5%, weigthings and LDA-based rebuildings being done at the same time.

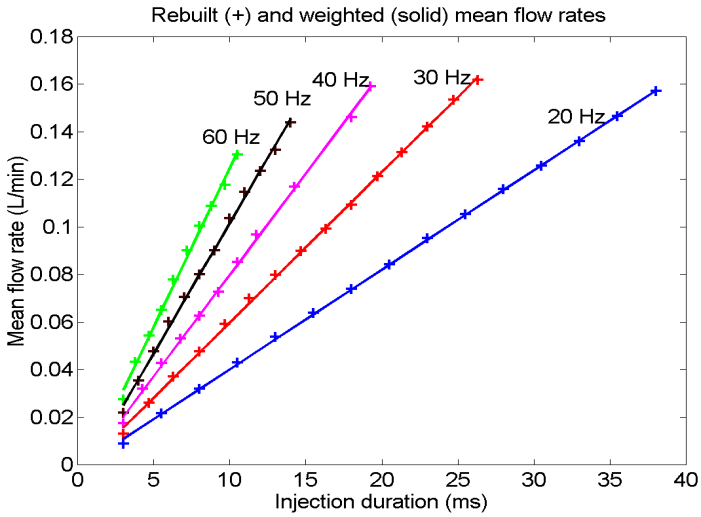

Fig. 9: Weigthed &. rebuilt mean flow rates

Finally, this method can also be dedicated to the transient analysis of unsteady sprays and is here applied to GDI sprays. Thanks to Particle Image Velocimetry, it has been possible to analyse the instantaneous air entrainment of a GDI spray (figure 10, [14]). We chose to compare the temporal evolution of the instantaneous liquid flow rate feeding the injector and the magnitude of the air velocity around the spray.

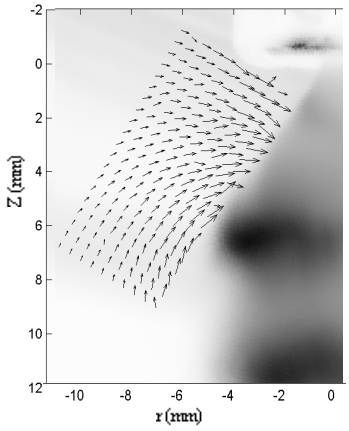

Fig. 10: Spray visualization and PIV 0.6 ms after starting of a 1.5 ms injection

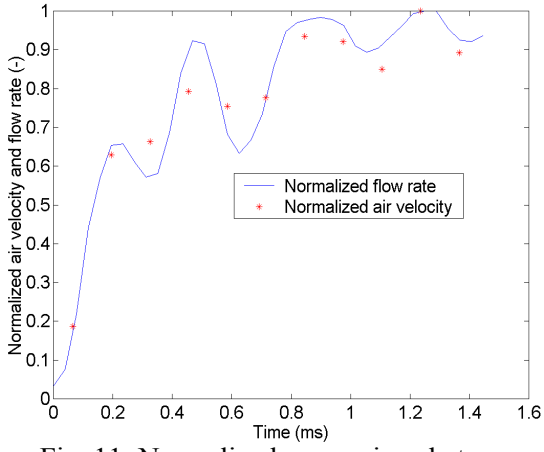

Fig. 11: Normalized comparison between rebuilt flow rate and air entrainment at Z=6mm

As we can see on figure 11, the air entrainment velocity roughly follows the dynamic of the injection. Indeed, even if the temporal discretisation is not accurate enough to fully validate this approach, the transient evolution is clearly put on light. We can also notice that acceleration phases are more corellated than decceleration ones but however noticeable. Further studies will be achieved to determine the transient air mass entrained by the spray.

6. Discussion

As already stressed in [1 ,2 ,4 ,5 ,6], this rebuilding method is well-suited to periodical unstationnary flows, and so, can be used to study gazoline or diesel injectors. Oscillations magnitudes are very important (up to 40% of the static flow rate) and their presence after

injection in the whole feeding loop has to be taken into account because of the considered frequencies.

Indeed, the state of the flow (velocity, acceleration) at the injection beginning will determine the maximum flow rate reached during injection. As a result, the coupling between two successive injections will not be the same for two different injection durations or frequencies. On figure 5, it is obvious that the 3 ms injection duration maximum flow rate is higher than the 1.5 ms. This is due to the injection while accelerating flow (for the 3ms injection duration) instead of decelerating one (for the 1.5 ms one).

Finally, it is now possible to determine the unsteady boundary conditions at the inlet of the injector, so giving access to more parameters while studying transient analysis of the spray development. It could also be interesting to monitor the spray fuel concentration evolution as a function of time (Laser Induced Fluorescence), as well as the time-dependant spray granulometry, to quantify their dependence to flow rate variations.

References :

[1] : Durst, F., M. Ismailov, et al. (1996). " Measurement of instantaneous flow rates in periodically operating injection systems. "
Experiments in fluids 20: 178-188

[2] : Bopp. S., Durst, F., Teufel M. and Weber H.. (1990). " Volumetric flow rate measurements in oscillating pipe flows with a laser Doppler sensor. ". Measurement science and technology, 1, : 917-923.

[3] : Lambossy, P. (1952). " Oscillations forcées d'un liquide incompressible visqueux dans un tube rigide et horizontal. Calcul de la force de frottement. " Helvetica Physiol. Acta, 371-386, 1.II.1952.

[4] : Durst, F., Melling A., Trimis, D. and Volkholz P. (1996). " Development of a flow meter for instantaneous flow rate measurements of anaesthetic liquids. ". Flow measurement instrumentation, vol. 7, n° ¾ : 215-221.

[5] : Ismailov M., Durst, F and Obokata T. (1999). " LDA flow rate measurements applied for analysis of transient injection characteristics. ". JSME international journal. Series B, fluids and thermal engineering, vol 42, n°1 , 22-29.

[6] : Ismailov M., Ishima T., Obokata T., Tsukagoshi M. and Kobayashi K. (1999). "Visualization and measurements of sub-millisecond transient spray dynamics applicable to direct injection gasoline engine (Part 3 :Measurements of instantaneous and integrated flow rates in high pressure injection system using LDA-based meter)". JSME international journal. Series B, fluids and thermal engineering, vol 442, n°1 , 22-29.

[7] : David M. Eckmann et James B. Grotberg (1991) " Experiments on transition to turbulence in oscillatory pipe flow. " Journal of Fluid Mechanics 222 : 329-350

[8] : Hino, M., M. Sawamoto, et al. (1976). " Experiments on transition to turbulence in an oscillatory pipe flow. " Journal of Fluid Mechanics 75 (2): 193-207

[9] : Vittori, G., R. Verzicco, (1997). " Direct simulations of transition in an oscillatory boundary layer. " Journal of Fluid Mechanics 75 (2): 193-207

[10] : Wu, X. (1992). " The nonlinear evolution of high-frequency resonant triad waves in an oscillatory Stokes layer at high Reynolds number. ". Journal of Fluid Mechanics 245 : 553-597

[11] : Wu, X., Lee, S. S. et Cowley, S.J. (1995). " On the weakly nonlinear three-dimensional instability of shear layers to pairs of oblique waves : the Stokes layer as a paradigm. ". Journal of Fluid Mechanics 253: 681-721

[13] : T. Poinsot and D. Veynante, "Theoretical and numerical combustion", Edwards.

[14] : Arbeau A, Bazile R, Ben L, Charnay G, Couteau G, Ferrand V & Jagu S, «Experimental study of air engulfment in a spray. Application to the set up of direct injection mixtures». Internal IMFT report.